Research Square

Preprints are preliminary reports that have not undergone peer review.
They should not be considered conclusive, used to inform clinical practice,
or referenced by the media as validated information.

Ruxolitinib acts as a selective inhibitor of CaMKII-γ to impede the progression of Bortezomib-resistant multiple myeloma through AMPK-ULK1 axis-mediated autophagy pathway

Mingdi Wang

WMD202503@163.com

Peking University Shougang Hospital

Ruqi Liang

Hong Liu

Yizhao Chen

Jianru Tian

Chaofeng Zhang

Article

Keywords: Bortezomib-resistant multiple myeloma, CaMKII-γ, high-throughput screening, selective small-molecule inhibitor, Ruxolitinib

Posted Date: October 10th, 2025

DOI: https://doi.org/10.21203/rs.3.rs-7490141/v1

License: This work is licensed under a Creative Commons Attribution 4.0 International License.
Read Full License

Additional Declarations: There is **NO** Competing Interest.

Abstract

Multiple myeloma (MM) has become the second most common hematologic malignancy. In recent years, the incidence rate of MM is increasing and the onset age of MM is ahead. Although proteasome inhibitors and other strategies play important roles in the treatment of MM, almost all patients develop resistance after treatment. Therefore, novel drug targets and innovative therapeutic strategies are greatly needed. Here, we identified calcium/calmodulin-dependent protein kinase II gamma (CaMKII-γ) as a potential therapeutic target for Bortezomib-resistant multiple myeloma (BRMM). Then mechanism exploration results showed that autophagy pathway via CaMKII-γ-AMPK-ULK1 axis mediated the progression of BRMM. Furthermore, we identified Ruxolitinib (IC_{50} = 109 nM) as a selective small-molecule inhibitor of CaMKII-γ through high-throughput screening (HTS). Ruxolitinib demonstrated significantly tumor-suppressive effects on BRMM both *in vitro* and *in vivo* via down-regulation of CaMKII-γ-AMPK-ULK1 axis-mediated autophagy pathway. Notably, the antit-umor effect of Ruxolitinib was comparable to that observed with genetic CaMKII-γ ablation, highlighting its potential as a novel therapeutic strategy for the treatment of BRMM.

Highlights

CaMKII-γ is a potential therapeutic target for BRMM.

Ruxolitinib is a selective small-molecule inhibitor of CaMKII-γ discovered by HTS.

Ruxolitinib is a potential drug for BRMM.

Introduction

Multiple myeloma (MM) has become the second most common hematologic malignancy with the infinite clonal proliferation of malignant plasma cells in the bone marrow and the secretion of monoclonal immunoglobulin. The symptoms include skeletal destruction, infections, anemia, hypercalcemia, and renal failure[1–2]. For the treatment of multiple myeloma, proteasome inhibitors (Bortezomib, Carfilzomib and Ixazomib) and other first-line strategies in clinics have prolonged the survival time of patients by 2–3 times. However, almost all patients develop resistance after treatment, leading to eventual treatment failure and recurrence, which severely affects the survival of MM patients[3–6]. Therefore, novel drug targets and innovative therapeutic strategies are in great need for drug-resistant MM patients.

CaMKII-γ is a member of CaMKII family (calcium/calmodulin-dependent protein kinase II), which belongs to serine/threonine kinase family. There are four subtypes in CaMKII family including CaMKII-α, CaMKII-β, CaMKII-γ and CaMKII-δ, regulated by calcium ions and calmodulin. Members of CaMKII family play important roles in signal transduction, neurotransmitter release, synaptic plasticity, gene regulation and other biological processes[7–8]. Numerous studies have shown that aberrant activation of CaMKII-γ is

closely related to a variety of tumors, such as T-cell lymphoma, myeloid leukemia and colon cancer[9–13]. In particular, studies also found that CaMKII-γ was aberrantly activated in MM and its expression level was positively correlated with malignant progression and poor prognosis, suggesting that CaMKII-γ could be a potential therapeutic target in MM. However, the relationship between CaMKII-γ and drug-resistant MM has not been reported, so in this study we explored whether CaMKII-γ is a potential therapeutic target in drug-resistant MM.

AMPK-ULK1 axis-mediated autophagy pathway is an important cellular self-protective and metabolic regulation mechanism, which not only maintains cell homeostasis, but also solves cell stress by degrading and recycling cell components, thereby preventing diseases and maintaining cell function. Multiple studies have shown that AMPK-ULK1 axis-mediated autophagy pathway plays a complex dual role in tumors. On the one hand, autophagy can promote the survival and proliferation of tumor cells; on the other hand, excessive autophagy will lead to resource depletion and inhibit tumor growth[14–15]. Importantly, studies have found that Bortezomib resistance is induced by activation of AMPK-ULK1 axis-mediated protective autophagy in MM cells, in which NCX 1/Ca^{2+} triggers the autophagy flux of MM cells through the non-classical NF-κB pathway, thereby reducing the sensitivity of MM to Bortezomib[16]. CaMKII, as an important regulator of Ca^{2+} signaling, has also been found to significantly enhance autophagy flux to protect cell survival under short-term starvation conditions. Therefore, we hypothesized that BRMM cells may also achieve cell survival by activating CaMKII-γ-AMPK-ULK1 axis to enhance autophagy pathway, which was verified in this study.

Ruxolitinib, as a small-molecule inhibitor of JAK1/2, is the first drug approved by the FDA for the treatment of moderate or high-risk myelofibrosis[17]. It mainly plays a variety of roles such as anti-inflammatory, immune regulation and inhibition of abnormal cell growth, which is widely used in the treatment of myelofibrosis, polycythemia vera, and corticosteroid-refractory acute graft-versus-host disease[18]. Recent studies have found that Ruxolitinib also has a role in reducing arthritis symptoms and cardiac protection[19].

Results

1. Overexpression of CaMKII-γ is associated with MM recurrence and poor prognosis.

Studies have revealed that dysregulation of CaMKII-γ (encoded by the *CAMK2G* gene) is closely associated with various hematological malignancies[10–13]. Previous studies have also found that CaMKII-γ was aberrantly activated in MM and its expression level was positively correlated with malignant progression and poor prognosis[10]. In order to explore whether CaMKII-γ is related to drug-resistant MM, we analyzed the MMRFCoMMpass database containing 764 bone marrow samples derived from MM patients and 80 bone marrow samples derived from recurrent MM patients. The result showed that compared with primary patients, the expression level of *CAMK2G* was significantly upregulated in recurrent patients (Fig. 1A). The further analysis result related to the survival of recurrent

MM patients showed that compared with recurrent MM patients with low *CAMK2G* expression, recurrent MM patients with high *CAMK2G* expression had shorter survival (Fig. 1B). Then to verify the results of the above bioinformatics analysis, we induced drug resistance in U266 and KMS11 cell lines using Bortezomib, the first-line clinical treatment drug for MM. Two Bortezomib-resistant cell lines, U266.BR and KMS11.BR, were obtained through the drug concentration escalation method, with IC_{50} values increased by 13.25-fold and 6.45-fold respectively (Fig. 1C-D). In both BRMM cell lines, we observed elevated CaMKII-γ protein levels compared to their non-resistant counterparts (Fig. 1E-F). To further validate the differential expression of CaMKII-γ in clinical samples, we performed immunohistochemical (IHC) staining on bone marrow tissue sections collected from healthy donors, newly diagnosed, and relapsed MM patients. The results revealed markedly elevated levels of CaMKII-γ protein in malignant plasma cells from relapsed MM patients compared to normal controls and newly diagnosed patients (Fig. 1G). Based on the above findings, we speculate that the abnormally high expression of CaMKII-γ may be closely related to the drug resistance and poor prognosis of MM.

2. CaMKII-γ is a potential target of BRMM.

To further address the role of CaMKII-γ in BRMM, we knocked down CaMKII-γ in U266.BR and KMS11.BR cells using siRNA (Fig. 2A-B). The result showed that knockdown of CaMKII-γ significantly inhibited the proliferation of BRMM (Fig. 2C-D). In addition to *in vitro* proliferation assays, we evaluated the tumor-suppressive effect of CaMKII-γ knockdown *in vivo* using a xenograft mouse model. BALB/c nude mice were subcutaneously injected with U266.BR cells transfected with either siRNA targeting CAMK2G (si-CAMK2G) or negative control siRNA (si-NC). Mice bearing si-CAMK2G tumors exhibited significantly slower tumor growth compared to the control group (Fig. 2E-G), while their body weight remained unaffected throughout the experimental period (Fig. 2H). Histological analysis of excised tumors showed a notable decrease in tumor cell density and increased necrosis in the si-CAMK2G group, as revealed by hematoxylin and eosin (H&E) staining. Furthermore, immunohistochemical staining for the proliferation marker Ki-67 demonstrated a markedly lower proliferation index in CaMKII-γ knockdown tumors relative to controls (Fig. 2I). These *in vivo* findings confirm the critical role of CaMKII-γ in sustaining BRMM tumor growth. In conclusion, CaMKII-γ is correlated with Bortezomib resistance in MM and represents a potential therapeutic target for the treatment of BRMM.

3. Autophagy pathway plays a key role in the regulation of BRMM.

To further explore the mechanism by which CaMKII-γ mediates drug-resistant MM, we conducted the GO (Gene Ontology) enrichment analysis on the MMRFCoMMpass database. The results revealed that compared with primary MM patients, the bone marrow samples of recurrent MM patients were significantly enriched in primary lysosomes, special granules and other cellular components closely related to autophagy (Fig. 3A). While compared with recurrent MM patients with low expression of CaMKII-γ, recurrent MM patients with high expression of CaMKII-γ had significantly enriched biological processes related to calcium signaling pathways, such as calcium-mediated signal transduction and positive regulation of cytoplasmic calcium ion concentration (Fig. 3B). To visualize the autophagic

activity at the cellular level, we performed monodansylcadaverine (MDC) staining to label autophagic vacuoles in U266.BR and KMS11.BR cells. Both cell lines were transfected with either si-CAMK2G or si-NC. The fluorescent signals representing autophagic vesicles were markedly reduced in CaMKII-γ knockdown cells compared to controls (Fig. 3C). This morphological evidence further confirmed that CaMKII-γ depletion suppressed autophagy in BRMM cells. Furthermore, earlier research has indicated that CaMKII promotes autophagic flux to mediate the drug resistance and maintain the survival of tumor cells [20–22]. Based on the above bioinformatics analysis results and relevant research reports, we speculate that CaMKII-γ may mediate the drug resistance of MM through regulating autophagy pathway. To further investigate the relationship between CaMKII-γ and autophagy in drug-resistant MM, we observed that si*CAMK2G*-mediated knockdown of CaMKII-γ led to a significant reduction of LC3-II protein level in BRMM (Fig. 3D-E). This finding suggests that the high level of autophagic flux in BRMM cells depend on the presence of CaMKII-γ. Autophagy is primarily regulated by AMPK activation and mTOR inhibition[23], with AMPK serving as a critical signaling molecule in the calcium-mediated pathway influencing autophagy[24]. Given this context, we examined the impact of CaMKII-γ on AMPK and its downstream targets. Western blotting analysis revealed that knockdown of CaMKII-γ not only reduced the phosphorylation levels of AMPK but also decreased the phosphorylation of ULK1 (Fig. 3F-G). These data indicate that CaMKII-γ plays a crucial role in the activation of AMPK-ULK1 axis-mediated autophagy signaling pathway in BRMM cells.

4. Ruxolitinib is a selective small-molecule inhibitor of CaMKII-γ

Despite KN-93 being recognized as a specific inhibitor of CaMKII[25], its inhibitory efficacy is suboptimal and it cannot differentiate between the four CaMKII isoforms. Consequently, there is an urgent need to develop selective inhibitors targeting CaMKII-γ. To address this, we established a HTS platform using recombinant CaMKII-γ protein to screen a library of 2,665 FDA-approved drugs for their potential to inhibit CaMKII-γ activity (Fig. 4A). In the initial screening, 8 compounds that inhibited CaMKII-γ activity by more than 80% at a concentration of 10 μM were identified (The complete HTS results are presented in Table S1). These compounds were then subjected to secondary screening to determine their half-maximal inhibitory concentrations (IC_{50}). Based on these results, we further evaluated their selectivity towards different CaMKII isoforms. Among these, Ruxolitinib (Fig. 4B) exhibited significant inhibitory activity against CaMKII-γ with an IC_{50} of 109 nM, along with notable isoform selectivity, demonstrating at least a 6-fold higher potency against CaMKII-γ compared to other isoforms (Fig. 4C-D). These findings suggest that Ruxolitinib could be a promising therapeutic agent for treating BRMM, thus warranting further investigation into its clinical utility in this context.

5. Ruxolitinib selectively inhibits CaMKII-γ via binding to its ATP-binding pocket.

To explore the interaction between Ruxolitinib and CaMKII-γ as well as to elucidate the underlying mechanism, molecular docking simulations were conducted to model the binding mode of Ruxolitinib to CaMKII-γ. The docking result indicated that the optimal docking pose of Ruxolitinib fitted well into the ATP-binding site, interacting with the V93 residue and C65 residue of CaMKII-γ through the formation of

two hydrogen bonds. At the same time, Ruxolitinib formed hydrophobic interactions with residues L20, V28, A41, V74, F90, L92, L143, L155, A156 and F158 of CaMKII-γ (Fig. 5A-C). These findings suggest that Ruxolitinib may inhibit the enzymatic activity of CaMKII-γ by competitively binding to its ATP-binding pocket.

6. Ruxolitinib inhibits the proliferation of BRMM cells by down-regulating autophagy pathway.

We have confirmed that Ruxolitinib is a potent and selective inhibitor of CaMKII-γ. To further investigate its effects on BRMM cells, we determined the IC_{50} values for U266.BR and KMS11.BR cells, which were 13.57 μM and 19.09 μM, respectively (Fig. 6A-B). In addition to biochemical validation, we used MDC staining to visualize autophagic vacuole formation after drug treatment. U266.BR and KMS11.BR cells were treated with 10 μM Ruxolitinib or vehicle (DMSO) for 24 hours and subjected to MDC staining. The results revealed that Ruxolitinib-treated cells displayed significantly fewer MDC-labeled autophagic vesicles compared to control cells (Fig. 6C), further supporting the conclusion that Ruxolitinib suppresses autophagy in BRMM cells through CaMKII-γ inhibition. While we have demonstrated that Ruxolitinib inhibits the proliferation of resistant cells, the precise mechanism by which it exerts this effect remains unclear. To elucidate the mechanism underlying Ruxolitinib's impact on the proliferation of BRMM cells, we treated the BRMM cells with 10 μM Ruxolitinib and observed no significant change in total CaMKII-γ levels, but a notable reduction in phosphorylated CaMKII-γ. Consistent with the knockdown results, the total levels of AMPK and ULK1 remained unchanged, while their phosphorylation levels were significantly reduced (Fig. 6D-E). Additionally, levels of the autophagy-related protein LC3-II were markedly decreased. These findings suggest that Ruxolitinib may inhibit the proliferation of BRMM cells via AMPK-ULK1 axis-mediated autophagy signaling pathway.

7. Ruxolitinib shows significantly anti-tumor activity against BRMM in vivo.

To evaluate the *in vivo* efficacy of Ruxolitinib on BRMM, we first established a xenograft model of BR human MM (U266.BR) cells in BALB/c nude mice (Fig. 7A). The results demonstrated that oral administration of Ruxolitinib exhibited remarkable anti-tumor activity in the resistant MM tumor model, specifically delaying tumor growth significantly starting from day 19 of treatment (Fig. 7B). In contrast, no significant changes in tumor growth rates were observed in the control group. Neither group showed significant weight loss during the study period (Fig. 7C). After a designated period, the mice were euthanized, and the tumors were excised for further analysis (Fig. 7D). Western blotting analysis of the tumor tissues confirmed the findings from the *in vitro* experiments. In U266.BR xenograft mice treated with Ruxolitinib, phosphorylation levels of CaMKII-γ were significantly reduced, and the phosphorylation levels of the autophagy-related proteins AMPK and ULK1, which indicate their activation, were also downregulated. Additionally, levels of the autophagy marker LC3-II were decreased, suggesting an overall reduction in autophagic flux (Fig. 7E). These results further indicate that Ruxolitinib can effectively treat BRMM by inhibiting CaMKII-γ. To assess the treatment's impact on tumor tissue, we performed H&E and Ki67 staining. The H&E results showed structural disruption and increased necrosis in the treatment group compared to the blank and control groups. Ki67 staining revealed markedly reduced proliferative

activity in the experimental group, aligning with the observed decrease in tumor volume (Fig. 7F). These immunohistochemical results are consistent with the observed reduction in tumor volume, confirming the treatment's inhibitory effect on tumor growth.

Discussion

In this study, CaMKII-γ was identified as a potential therapeutic target for the treatment of BRMM. Our results showed that the expression level of CaMKII-γ was significantly elevated in BRMM cells and the silencing of CaMKII-γ via si-RNA significantly inhibited the proliferation of BRMM cells. We also found that the autophagy pathway mediated via CaMKII-γ-AMPK-ULK1 axis regulated the proliferation of BRMM cells and verified by western blotting. Then through high-throughput screening, we identified Ruxolitinib, a small-molecule inhibitor with high selectivity to CaMKII-γ among 2,665 compounds, which effectively inhibited the proliferation of BRMM both *in vitro* and *in vivo* by suppressing the autophagy pathway via CaMKII-γ-AMPK-ULK1 axis. Moreover, molecular docking simulation was employed to elucidate the interaction mechanism between Ruxolitinib and CaMKII-γ. Our findings suggest that Ruxolitinib, an FDA-approved drug, can be repurposed as a selective CaMKII-γ inhibitor for the treatment of BRMM, offering a promising therapeutic strategy. This research highlights the importance of identifying novel therapeutic targets and developing targeted therapies to improve the outcomes for BRMM patients.

One limitation of this study is the binding mode of Ruxolitinib and CaMKII-γ was obtained by molecular docking simulations, which is not exact enough. Future studies can perform X-ray diffraction to resolve the true co-crystal structure of Ruxolitinib and CaMKII-γ. Another limitation of the current work is the reliance on subcutaneous tumor models. Although these models offer practical advantages for measuring tumor volume and response, they lack the anatomical and physiological context of the original tissue, which can influence drug delivery, immune infiltration, and metastatic behavior. To overcome this constraint and strengthen the translational impact of our research, subsequent investigations will utilize orthotopic implantation models to achieve a more faithful representation of human disease.

For the treatment of MM, drug resistance remains a significant challenge, with mechanisms including gene mutations, epigenetic alterations and influences from the tumor microenvironment [26]. Although traditional chemotherapy remains the primary treatment, its efficacy is limited. And novel therapeutic strategies such as chimeric antigen receptor T-cell (CAR-T) therapy, monoclonal antibody therapy and bispecific antibody therapy have shown promising results in clinical treatment[27–29]. Future research will focus on elucidating resistance mechanisms, developing new targeted drugs, and optimizing combination therapy strategies to improve treatment outcomes and survival rates for the patients of drug-resistant MM.

Methods and Materials

Bioinformatic analysis

To investigate the correlation between CaMKII-γ and BRMM, we used R4.3.2 for statistical analysis and examined bone marrow sample data of MM patients from the MM Research Foundation CoMMpass database (MMRFCoMMpass), which includes bone marrow microarray data from 764 primary MM patients and 80 recurrent MM patients. The analyzed data consisted of RNA-seq and clinical data (overall survival). Firstly, we grouped the patients in the dataset and performed log2 conversion on the expression level of *CAMK2G*. Subsequently, we used the "ggplot2" package to draw violin plots, and "ggpubr" was used to add statistical significance markers to assess the differential expression levels of *CAMK2G* in different patient groups. Meanwhile, overall survival analysis of high and low expression of *CAMK2G* was conducted on recurrent MM patients, with the median expression level set as the threshold, and the samples were divided into high expression group and low expression group. Furthermore, the ‘survfit’ function of the "Survival" package was used to analyze the survival differences between the two groups, and the log-rank test method was used to evaluate the significance of survival differences between samples from different groups.

To explore the mechanism by which CaMKII-γ mediates BRMM, we conducted statistical analysis using R 4.3.2 and examined bone marrow sample data of recurrent MM patients from the MM Research Foundation CoMMpass database (MMRFCoMMpass). Firstly, a differential expression analysis method based on linear models was adopted to identify the genes with significantly differential expression between the recurrent group and the primary group using "limma". The target comparison group was defined using the ‘makeContrasts’ function to quantify the expression differences between the two groups. The ‘lmFit’ function was employed to conduct linear regression modeling on the gene expression matrix, correlating the expression levels with the grouping variables. Using the ‘eBayes’ function to conduct “Empirical Bayes moderation” on the residual variance of the model, thereby enhancing the robustness of variance estimation in small sample data. The adjusted P-value was less than 0.05, which was used to control the false positive rate in multiple comparisons. Based on the strict criteria mentioned above, we identified 995 genes with significant differences in recurrent MM bone marrow samples. To further explore the functions of these differentially expressed genes, we conducted GO enrichment analysis using the ‘enrichGO’ function of the "clusterProfiler" package. Subsequently, the differentially expressed genes were mapped to the GO database to calculate the significance of enrichment for each type of function. To visually display the results of GO enrichment analysis, we adopted the ‘dotplot’ function to draw the bubble chart, thereby facilitating the identification of functional genes closely related to recurrent MM patients. Then, we used the ‘read’ function to load the preprocessed expression matrix. To ensure data reliability, the first column gene names were set as matrix row names using the "row. names=1" parameter, resulting in a standardized expression matrix. Using the median expression value of *CAMK2G* as the threshold, the samples were divided into the high-expression group and the low-expression group. And factor-type variables were adopted for grouping, which was used for subsequent difference analysis. A framework for differential analysis was constructed based on the “linear model”. The linear model was fitted by the ‘lmFit’ function of the "limma" package and Bayesian smoothing correction was performed by the ‘eBayes’ function. To analyze the biological functions of differentially expressed genes, based on the above differential gene analysis,

we subsequently used the ‘enrichGO’ function of the "clusterProfiler" package for GO enrichment analysis. In order to visually display the results of GO enrichment analysis, we also generated the bubble chart using the ‘dotplot’ function to help identify functional genes closely related to high expression of *CAMK2G* in recurrent MM patients.

Cell Culture

The KMS11, U266 cell lines were obtained from American Type Culture Collection (ATCC), and cultured in RPMI 1640 medium (Cytiva, Cat#SH30022.01) containing 10% fetal bovine serum (Gibco, Cat#10099141C) and 1% Penicillin-Streptomycin Solution (Gibco, Cat#15140122). All cells were incubated at 37℃ with 5% CO_2.

Establishment of drug-resistant cell line

We selected U266 and KMS11 cells that were in the logarithmic growth phase and placed them in RPMI 1640 complete medium containing the first-line treatment drug for multiple myeloma, Bortezomib. The concentration gradient of Bortezomib was set at 5, 10, 20, 40, 80, and 160 nM, starting from the lowest concentration of 5 nM and increasing in a stepwise manner. After treating the cells with Bortezomib for 24 hours, Bortezomib was removed and replaced with fresh complete medium, and the cells were continued to be cultured. Then, the concentration of Bortezomib was gradually increased, usually once every 4 weeks. In the Bortezomib medium at a concentration of 160 nM, the cells proliferated stably and were identified as drug-resistant cell lines, named U266.BR and KMS11.BR respectively.

Western blotting analysis

Cell specimens were washed three times with PBS, and total cellular protein was extracted using RIPA buffer (Radio-Immunoprecipitation Assay buffer) (Servicebio, Cat#G2002). Cell extracts were subjected to sodium dodecyl sulfate–polyacrylamide gel electrophoresis (SDS-PAGE; 10% polyacrylamide gels), and then transferred to polyvinylidene difluoride (PVDF) membranes (Servicebio, Cat#G6044-0.45) and blocked with Protein Free Rapid Blocking Buffer (Servicebio, Cat#G2052). The membranes were then incubated with primary antibodies overnight at 4℃. After washing three times with TBST, membranes were incubated with a horseradish peroxidase-conjugated secondary antibody at room temperature for 2 h, and detected with Super-Sensitive ECL chemiluminescent substrate (Biosharp, Cat#BL520A). The antibodies used were described before. Quantification of western blotting was performed using the ImageJ software.

The antibodies are as follows: CaMKII-γ (Abcam, Cat#AB201966, 1:2,000); p-CaMKII-γ (CST, Cat#181602, 1:1,000); GAPDH (Abcam, Cat#AB181602, 1:12,000); p-ULK1 (Ser555) (CST, Cat#5869, 1:1,000); ULK1 (CST, Cat#8054, 1:1,000); p-AMPK (Thr172) (CST, Cat#2535, 1:1,000); AMPK (CST, Cat#5831, 1:1,000); LC3-II (CST, Cat#2775, 1:1,000); Goat Anti-Mouse IgG H&L (HRP) (Abcam, Cat#AB205719, 1:20,000); Goat Anti-Rabbit IgG H&L (HRP) (Abcam, Cat#AB205718, 1:20,000).

Immumohistochemical Staining

Formalin-fixed paraffin-embedded (FFPE) bone marrow biopsy tissues from healthy donors, newly diagnosed and relapsed MM patients, as well as xenograft tumor tissues from different treatment groups, were sectioned at 4 μm thickness. Healthy donors, newly diagnosed and relapsed MM patients tissues were purchased from Shanghai YEPCOME Biotechnology Co., Ltd. Sections were first deparaffinized with xylene, rehydrated through a graded ethanol series, and subjected to histological or immunohistochemical staining as follows.

For hematoxylin and eosin (H&E) staining, slides were stained with hematoxylin for 5 minutes and eosin for 2 minutes, followed by dehydration and mounting with neutral resin. H&E staining was used to evaluate tissue morphology and necrotic regions in xenograft tumor samples, including those from mice injected with si-CAMK2G-transfected cells and mice treated with Ruxolitinib.

For immunohistochemistry (IHC), antigen retrieval was performed in 0.01 M sodium citrate buffer (pH 6.0) at 95–100°C for 15 minutes. Endogenous peroxidase activity was blocked with 3% hydrogen peroxide for 10 minutes. After blocking with 5% bovine serum albumin (BSA) for 30 minutes, slides were incubated overnight at 4°C with the following primary antibodies: anti-CaMKII-γ (Abcam, Cat#AB201966, 1:200) for patient bone marrow tissues, and anti-Ki-67 (CST, Cat#9449, 1:400) for tumor tissues. Subsequently, slides were incubated with HRP-conjugated secondary antibodies (Abcam, Cat#AB205718, 1:500) for 30 minutes at room temperature. Detection was performed using DAB (3,3'-diaminobenzidine) substrate, and nuclei were counterstained with hematoxylin.

All stained sections were visualized using a light microscope. Immunohistochemical evaluation was performed by two independent pathologists blinded to the experimental groups. The immunoreactivity score was calculated based on the proportion of positively stained cells and the staining intensity.

MDC Staining

To visualize autophagic activity in BRMM cells, monodansylcadaverine (MDC) staining was performed using the MDC Autophagy Detection Kit (Beyotime, Cat#C3018S) according to the manufacturer's instructions. Two experimental conditions were applied in U266.BR and KMS11.BR cells: (1) CaMKII-γ knockdown using si-CAMK2G, and (2) Ruxolitinib treatment (10 μM for 24 h), with corresponding negative controls.

For suspension cell staining, 5×10^5 cells per group were collected by centrifugation at 500 × g for 5 minutes at room temperature and washed once with PBS. Cells were resuspended in 1 mL working MDC staining solution (prepared by diluting 1000× MDC stock 1:1000 with 1× Assay Buffer) and incubated at 37°C for 30 minutes in the dark. Following incubation, cells were washed three times with 1× Assay Buffer (1 mL each time) and then resuspended in 1 mL Assay Buffer for imaging.

Stained cells were smeared on glass slides and immediately examined under a fluorescence microscope using a UV excitation filter set (excitation wavelength 335 nm; emission 512 nm). MDC-labeled autophagic vacuoles appeared as distinct punctate green fluorescence in the cytoplasm. For all

experiments, staining and imaging were performed under minimal light exposure to reduce photobleaching. Negative controls were included and processed in parallel.

RNA Interference Analysis

The specific CaMKII-γ small interfering RNA (siRNA) were synthesized by Guangzhou RiboBio Co. Ltd. Cells were plated into 6-well plates at 6 x 10^5 cells/well, and then transfected with each density of 100 nM CaMKII-γ siRNA or scrambled negative siRNA using Lipofectamine 3000 Reagent (Invitrogen, Cat#11668030), according to the manufacturer's instructions. The medium was replaced 24 h post-transfection, and the cells were cultured in fresh medium. Cells were harvested at 72 h post-transfection. The success of the siRNA transfection was confirmed by demonstrating the inhibition of CaMKII-γ protein expression.

High-throughput screening for CaMKII-γ inhibitors

To discover new CaMKII-γ inhibitors as potential treatments for BRMM, we established a screening system using recombinant CaMKII-γ protein to test the inhibitory effects of FDA-approved drug library containing 2665 FDA-approved drugs (Obtained from MedChemExpress (MCE)). After initial screening and secondary activity validation, we identified an inhibitor named Ruxolitinib, which effectively inhibits CaMKII-γ protein activity. Subsequently, we used human BRMM cells overexpressing CaMKII-γ to further analyze the effects of Ruxolitinib on human BRMM cells. Our results indicate that Ruxolitinib can reduce CaMKII-γ activity, decrease CaMKII-γ-induced human BRMM cell death, suggesting that it may be a significant inhibitor.

Kinase Activity Assay

For the inhibitor screening, the CaMKII-γ kinase activity assay was performed as follows. When CaMKII-γ was activated, it phosphorylated substrates with converting ATP to ADP. In this assay, the phosphorylation of a peptide substrate (autocamtide-3) of CaMKII-γ was enzymatically coupled to the transition of ATP to ADP. The ADP-Glo® Kinase Assay reagent was used to stop kinase reaction and remove unreacted ATP. After adding kinase detection reagent to stop ATP depletion reaction and convert ADP to ATP, ATP was further converted to light by luciferase reaction (Promega, Cat#V9102).

Kinase Activity Assay of CaMKII-γ was accomplished by incubating 2 ng/μL CaMKII-γ recombinant protein with 0.2 mM $CaCl_2$, 10 mM $MgCl_2$, 0.01 mM ATP (Promega, Cat#V9102), 200 μM autocamtide-3 (KKALHRQETVDAL), 30 nM CaM (Sigma, Cat#C4874), and 0.1 mg/mL BSA (Albumin from bovine serum) in a buffer containing 25 mM Tris-HCl pH 7.5. The blank reaction contained all the above components except ATP. The kinase reaction was allowed to run for 30 minutes at room temperature (25-27℃), and ADP-Glo® Kinase Assay reagent Used according to the instructions from Promega. Human CaMKII-γ recombinant protein was produced by Readcrystal. Autocamtide-3 was produced by BioAct Peptide Biotechnology LLC.

Cell viability assay

To verify the resistance of BRMM cell lines to Bortezomib, we seeded U266, U266.BR, KMS11 and KMS11.BR cells at 8,000 cells/well in 96-well plates, and treated with Bortezomib to obtain cell viability levels at different concentrations.

To verify whether knocking down of CaMKII-γ inhibits the proliferation of BRMM, we seeded 2,000 BRMM cells/well MM cells for 5 days and detect the cell viability level every day.

To verify the inhibitory activity of Ruxolitinib on the proliferation of BRMM cells, we seeded U266.BR cells and KMS11.BR cells at 8,000 cells/well in 96-well plates and treated them with DMSO or Ruxolitinib for 48 h. Then we add 100 μL CellTiter-Glo® Luminescent Cell Viability Assay reagent (Promega, Cat#G9243) to each well and incubate the plates in Microporous Quick Shaker for 10 min. The incubated 96-well plate was placed on the microplate reader to get the cell viability level.

Xenograft mouse model

The experimental procedures and animal protocols were approved by Bioscience and Medical Ethics Committee of Taiyuan University of Technology. The temperature and humidity of the animal room are maintained at 20-26℃ and 40%-70%, respectively. All mice were given 12 h of light and 12 h of darkness in turn each day. BALB/c nude mice were purchased from Huachuang Sino Laboratory Animals Co. Ltd.

To establish xenograft models, U266.BR cells in the logarithmic growth phase were resuspended in PBS:Matrigel (1:1) and subcutaneously injected into the right groin of each mouse (1.5×10^7 cells in 0.1 mL PBS mixed with 0.1 mL Matrigel).

Two experimental models were established as follows: 1.siRNA knockdown model: U266.BR cells were transfected with either siRNA targeting CAMK2G (si-CAMK2G) or scrambled control siRNA (si-NC) for 72 h prior to injection. Mice (n = 5 per group) received no further intervention. Tumor growth was monitored to assess the in vivo effects of CaMKII-γ knockdown. 2.Drug treatment model: Mice injected with untreated U266.BR cells were randomly assigned to two groups (n = 5 per group) when tumors reached 100 mm^3. The treatment group received intraperitoneal injections of Ruxolitinib (60 mg/kg in 0.25 mL saline) every other day, while the control group received an equal volume of 0.9% saline following the same schedule. Tumor volumes and body weight were measured once every two days.

Statistics and reproducibility

Data were expressed as mean ± SD. Statistical analysis was performed using GraphPad Prism 8 software. For experiments with two groups, two-tailed Student's t test was used. $P < 0.05$ was considered statistically significant. As indicated in the figure legends, all in vitro experiments were performed in three biological replicates unless stated otherwise. Representative micrographs and western blotting shown in figures were repeated three times independently with similar results.

Declarations

Acknowledgments

The National Science Foundation of Shanxi Province [grant number 202303021212068]; the Science and Technology Innovation Project of Shanxi Province [grant number RD2300004063]; and the Research Start-up Foundation of Taiyuan University of Technology [grant number RY2400000585].

Declaration of interest

The authors declare that a patent application related to the methodology and result described in this study has been filed. Ruqi Liang and Chaofeng Zhang are listed as inventors. The application is currently pending and has not yet been published. No further conflicts of interest are declared.

Ethical Statement

Approval of the research protocol by an Institutional Reviewer Board: N/A.

Informed Consent: N/A.

Registry and the Registration No. of the study/trial: N/A.

Animal Studies: All animal procedures were conducted in strict accordance with the guidelines of the Ethics Committee of the School of Biological and Medical Sciences at Taiyuan University of Technology and complied with relevant national and international regulations concerning animal welfare and ethics.

Author Contrbutions

The work reported in the article has been performed by the authors, unless clearly specified in the text. R.Q.L. designed the study. R.Q.L. and H.L. performed the screening. H.L. performed the gene validation and cell culture studies. H.L. performed the experiment on mice. Y.Z.C. performed bioinformatic analysis and molecular simulation docking. J.R.T. conducted data analysis. R.Q.L. secured funding and resources for the studies. R.Q.L. wrote the first draft, M.D.W. and C.F.Z. revised the paper, while all the other authors provided comments.

Data Availability Statement

Data sources and handling of the publicly available datasets used in this study are described in the Materials and Methods. Further details and other data that support the findings of this study are available from the corresponding authors upon request.

Corresponding author

Correspondence to Mingdi Wang and Chaofeng Zhang

References

1. van de Donk NWCJ, Pawlyn C, Yong KL. Multiple myeloma. Lancet. 2021 Jan 30;397(10272):410-427.
2. Wittner J, Schuh W. Krüppel-like factor 2: a central regulator of B cell differentiation and plasma cell homing. Front Immunol. 2023 May 12;14:1172641.
3. Salama Y, Heida AH, Yokoyama K, Takahashi S, Hattori K, Heissig B. The EGFL7-ITGB3-KLF2 axis enhances survival of multiple myeloma in preclinical models. Blood Adv. 2020 Mar 24;4:1021-1037.
4. Hideshima T, Ikeda H, Chauhan D, Okawa Y, Raje N, Podar K, Mitsiades C, Munshi NC, Richardson PG, Carrasco RD, Anderson KC. Bortezomib induces canonical nuclear factor-kappaB activation in multiple myeloma cells. Blood. 2009 Jul 30;114:1046-1052.
5. Scott K, Hayden PJ, Will A, Wheatley K, Coyne I. Bortezomib for the treatment of multiple myeloma. Cochrane Database Syst Rev. 2016 Apr 20;4:CD010816.
6. Dutta D, Liu J, Wen K, Kurata K, Fulciniti M, Gulla A, Hideshima T, Anderson KC. BCMA-targeted bortezomib nanotherapy improves therapeutic efficacy, overcomes resistance, and modulates the immune microenvironment in multiple myeloma. Blood Cancer J. 2023 Dec 11;13(1):184.
7. Wang YY, Zhao R, Zhe H. The emerging role of CaMKII in cancer. Oncotarget. 2015 May 20;6(14):11725-34.
8. Yasuda R, Hayashi Y, Hell JW. CaMKII: a central molecular organizer of synaptic plasticity, learning and memory. Nat Rev Neurosci. 2022 Nov;23(11):666-682.
9. He Q, Li Z. The dysregulated expression and functional effect of CaMK2 in cancer. Cancer Cell Int. 2021 Jun 30;21(1):326.
10. Yang L, Wu B, Wu Z, Xu Y, Wang P, Li M, Xu R, Liang Y. CAMKIIγ is a targetable driver of multiple myeloma through CaMKIIγ/ Stat3 axis. Aging (Albany NY). 2020 Jul 13;12(13):13668-13683.
11. Gu Y, Chen T, Meng Z, Gan Y, Xu X, Lou G, Li H, Gan X, Zhou H, Tang J, Xu G, Huang L, Zhang X, Fang Y, Wang K, Zheng S, Huang W, Xu R. CaMKII γ, a critical regulator of CML stem/progenitor cells, is a target of the natural product berbamine. Blood. 2012 Dec 6;120(24):4829-39.
12. Gu Y, Zheng W, Zhang J, Gan X, Ma X, Meng Z, Chen T, Lu X, Wu Z, Huang W, Xu R. Aberrant activation of CaMKIIγ accelerates chronic myeloid leukemia blast crisis. Leukemia. 2016 Jun;30(6):1282-9.
13. Gu Y, Zhang J, Ma X, Kim BW, Wang H, Li J, Pan Y, Xu Y, Ding L, Yang L, Guo C, Wu X, Wu J, Wu K, Gan X, Li G, Li L, Forman SJ, Chan WC, Xu R, Huang W. Stabilization of the c-Myc Protein by CAMKIIγ Promotes T Cell Lymphoma. Cancer Cell. 2017 Jul 10;32(1):115-128.e7.
14. Li X, He S, Ma B. Autophagy and autophagy-related proteins in cancer. Mol Cancer. 2020 Jan 22;19:12.
15. Levy JMM, Towers CG, Thorburn A. Targeting autophagy in cancer. Nat Rev Cancer. 2017 Sep;17:528-542.

16. Li T, Xiao P, Qiu D, Yang A, Chen Q, Lin J, Liu Y, Chen J, Zeng Z. NCX1/Ca2+ promotes autophagy and decreases Bortezomib activity in multiple myeloma through non-canonical NFκB signaling pathway. Cell Commun Signal. 2024 May 6;22:258.
17. Harrison C, Kiladjian JJ, Al-Ali HK, Gisslinger H, Waltzman R, Stalbovskaya V, McQuitty M, Hunter DS, Levy R, Knoops L, Cervantes F, Vannucchi AM, Barbui T, Barosi G. JAK inhibition with Ruxolitinib versus best available therapy for myelofibrosis. N Engl J Med. 2012 Mar 1;366:787-98.
18. Becker H, Engelhardt M, von Bubnoff N, Wäsch R. Ruxolitinib. Recent Results Cancer Res. 2014;201:249-57.
19. Reyes Gaido OE, Pavlaki N, Granger JM, Mesubi OO, Liu B, Lin BL, Long A, Walker D, Mayourian J, Schole KL, Terrillion CE, Nkashama LJ, Hulsurkar MM, Dorn LE, Ferrero KM, Huganir RL, Müller FU, Wehrens XHT, Liu JO, Luczak ED, Bezzerides VJ, Anderson ME. An improved reporter identifies Ruxolitinib as a potent and cardioprotective CaMKII inhibitor. Sci Transl Med. 2023 Jun 21;15:7839.
20. Patergnani S, Danese A, Bouhamida E, Aguiari G, Previati M, Pinton P, Giorgi C. Various Aspects of Calcium Signaling in the Regulation of Apoptosis, Autophagy, Cell Proliferation, and Cancer. Int J Mol Sci. 2020 Nov 6;21:8323.
21. Sukumaran P, Nascimento Da Conceicao V, Sun Y, Ahamad N, Saraiva LR, Selvaraj S, Singh BB. Calcium Signaling Regulates Autophagy and Apoptosis. Cells. 2021 Aug 18;10:2125.
22. Zhan Q, Jeon J, Li Y, Huang Y, Xiong J, Wang Q, Xu TL, Li Y, Ji FH, Du G, Zhu MX. CAMK2/CaMKII activates MLKL in short-term starvation to facilitate autophagic flux. Autophagy. 2022 Apr;18:726-744.
23. Guo H, Ouyang Y, Yin H, Cui H, Deng H, Liu H, Jian Z, Fang J, Zuo Z, Wang X, Zhao L, Zhu Y, Geng Y, Ouyang P. Induction of autophagy via the ROS-dependent AMPK-mTOR pathway protects copper-induced spermatogenesis disorder. Redox Biol. 2022 Feb 30;49:102227.
24. Jing Z, He X, Jia Z, Sa Y, Yang B, Liu P. NCAPD2 inhibits autophagy by regulating Ca2+/CAMKK2/AMPK/mTORC1 pathway and PARP-1/SIRT1 axis to promote colorectal cancer. Cancer Lett. 2021 Nov 1;520:26-37.
25. Gao L, Blair LA, Marshall J. CaMKII-independent effects of KN93 and its inactive analog KN92: reversible inhibition of L-type calcium channels. Biochem Biophys Res Commun. 2006 Jul 14;345:1606-10.
26. Gu LF, Cui XG, Cao XM, Chen SP. [Drug-Resistant Mechanism of Multiple Myeloma and Its Therapy Combined with HDACi -Review]. Zhongguo Shi Yan Xue Ye Xue Za Zhi. 2017 Apr;25:608-612.
27. Sun F, Cheng Y, Wanchai V, Guo W, Mery D, Xu H, Gai D, Siegel E, Bailey C, Ashby C, Al Hadidi S, Schinke C, Thanendrarajan S, Ma Y, Yi Q, Orlowski RZ, Zangari M, van Rhee F, Janz S, Bishop G, Tricot G, Shaughnessy JD Jr, Zhan F. Bispecific BCMA/CD24 CAR-T cells control multiple myeloma growth. Nat Commun. 2024 Jan 19;15:615.
28. Sonneveld P, Dimopoulos MA, Boccadoro M, Quach H, Ho PJ, Beksac M, Hulin C, Antonioli E, Leleu X, Mangiacavalli S, Perrot A, Cavo M, Belotti A, Broijl A, Gay F, Mina R, Nijhof IS, van de Donk NWCJ, Katodritou E, Schjesvold F, Sureda Balari A, Rosiñol L, Delforge M, Roeloffzen W, Silzle T, Vangsted A,

Einsele H, Spencer A, Hajek R, Jurczyszyn A, Lonergan S, Ahmadi T, Liu Y, Wang J, Vieyra D, van Brummelen EMJ, Vanquickelberghe V, Sitthi-Amorn A, de Boer CJ, Carson R, Rodriguez-Otero P, Bladé J, Moreau P; PERSEUS Trial Investigators. Daratumumab, Bortezomib, Lenalidomide, and Dexamethasone for Multiple Myeloma. N Engl J Med. 2024 Jan 25;390:301-313.

29. Rajkumar SV. Multiple myeloma: 2024 update on diagnosis, risk-stratification, and management. Am J Hematol. 2024 Sep;99:1802-1824.

Figures

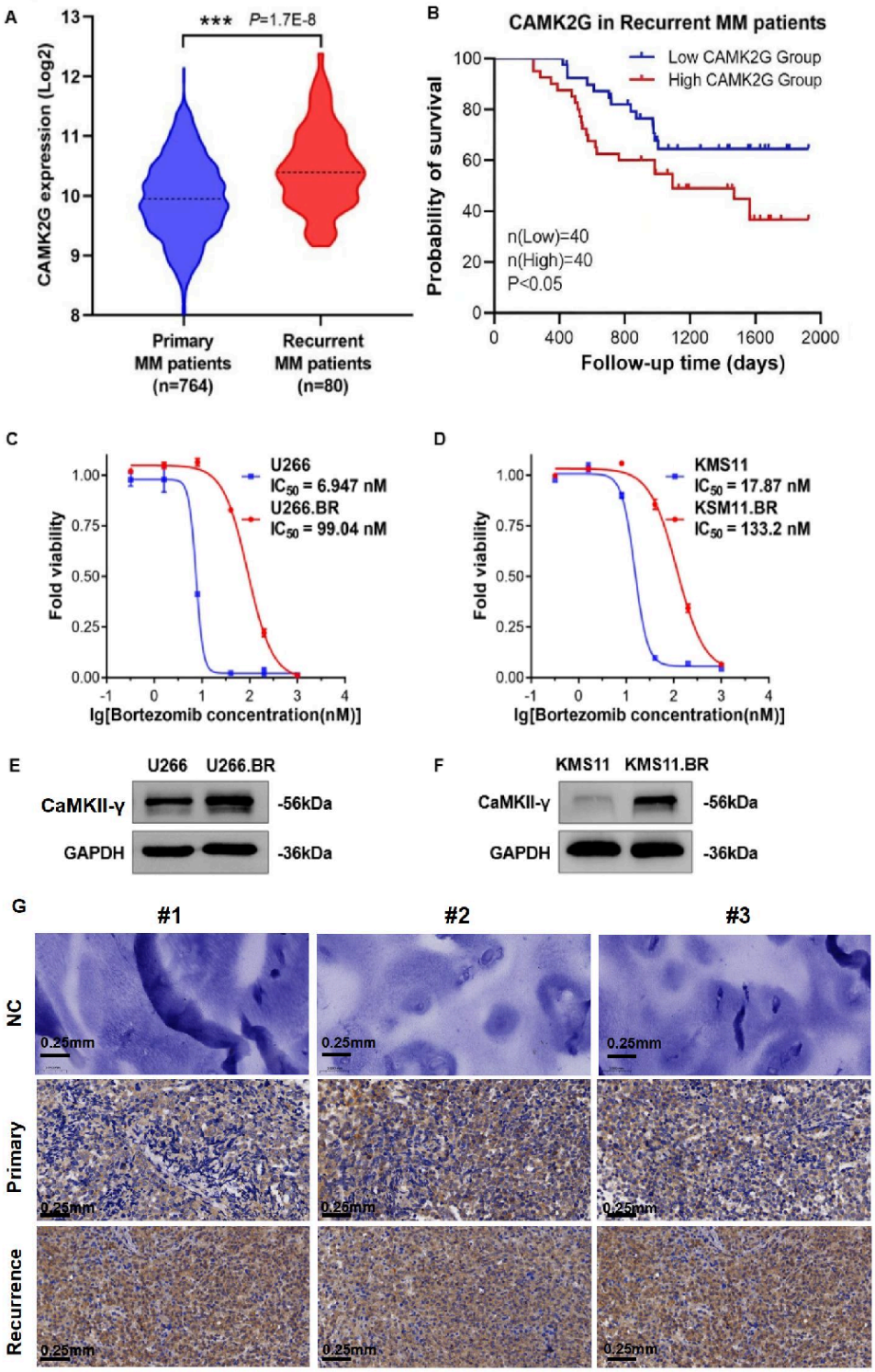


Figure 1

Overexpression of CaMKII-γ is associated with MM recurrence and poor prognosis. (A) MMRFCoMMpass database was utilized to compare CAMK2G expression level between primary and recurrent MM patients. **(B)** Kaplan-Meier curves depicted overall survival (OS) in recurrent MM patients stratified by CAMK2G expression levels. Statistical significance was assessed using the log-rank (Mantel-Cox) test. **(C-D)** MM cell lines (U266 and KMS11) and BRMM cell lines (U266.BR and KMS11.BR)

were treated with the indicated concentrations of Bortezomib for 48 h to test their IC_{50} values against Bortezomib. **(E-F)** Comparison of CaMKII-γ expression levels in MM cell lines (U266 and KMS11) and BRMM cell lines (U266.BR and KMS11.BR) tested by western blotting. **(G)** Representative immunohistochemical staining of CaMKII-γ in bone marrow tissues from normal controls, newly diagnosed and relapsed MM patients, showing elevated CaMKII-γ expression in relapsed samples.

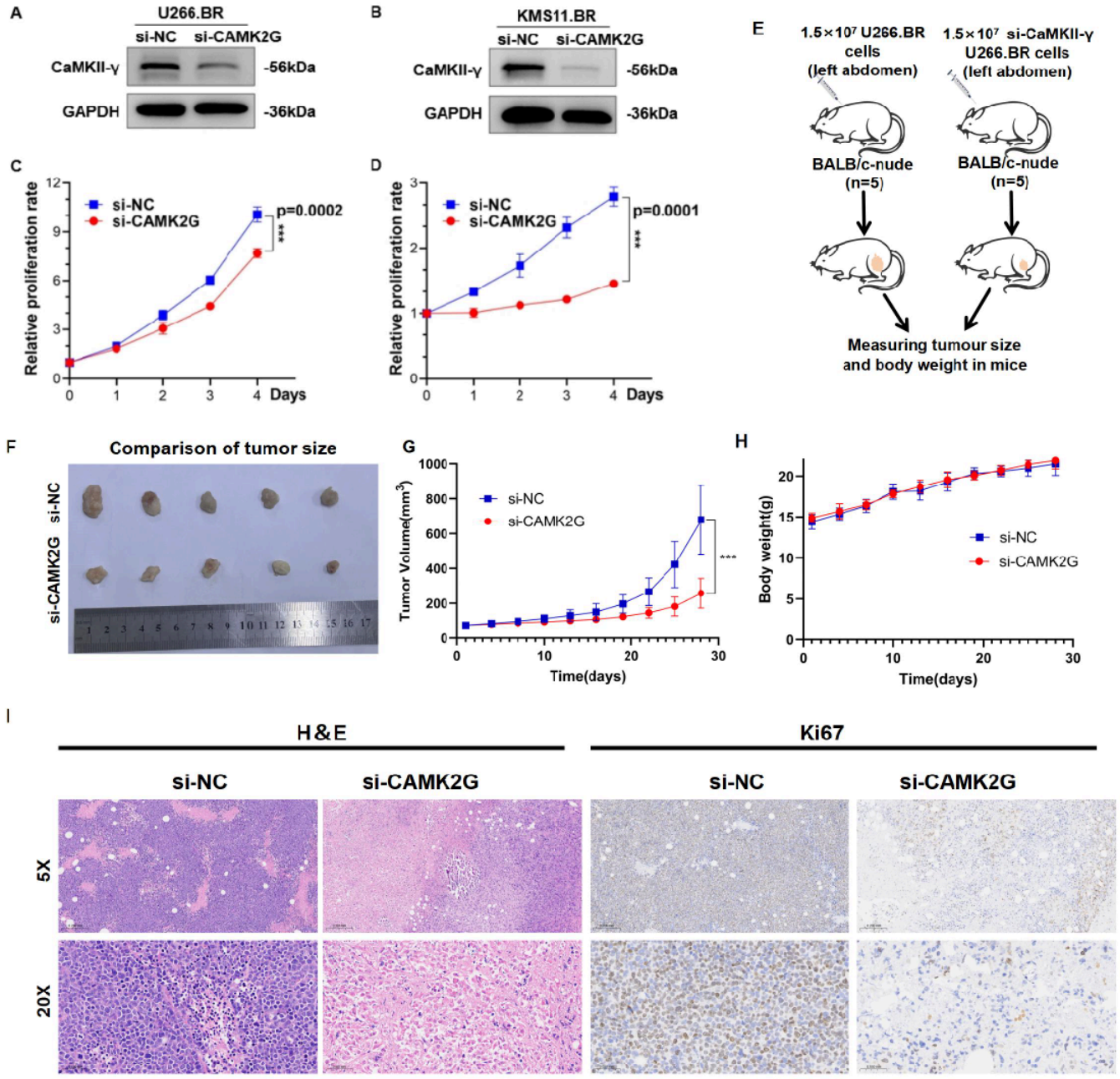


Figure 2

CaMKII-γ is a potential target of BRMM. (A-B) Comparison of CaMKII-γ expression levels in BRMM cell lines (U266.BR and KMS11.BR) transfected with si-NC and si-CAMK2G. **(C-D)** Comparison of cell proliferation activities in BRMM cell lines (U266.BR and KMS11.BR) transfected with si-NC and si-

CAMK2G. **(E-G)** Tumor volume growth curves of BALB/c nude mice injected with U266.BR cells transfected with si-NC or si-CAMK2G. **(H)** Body weight monitoring in both groups throughout the study period. **(I)** Representative H&E and Ki-67 immunohistochemical staining of tumor sections, showing decreased tumor cell density and proliferation in the si-CAMK2G group.

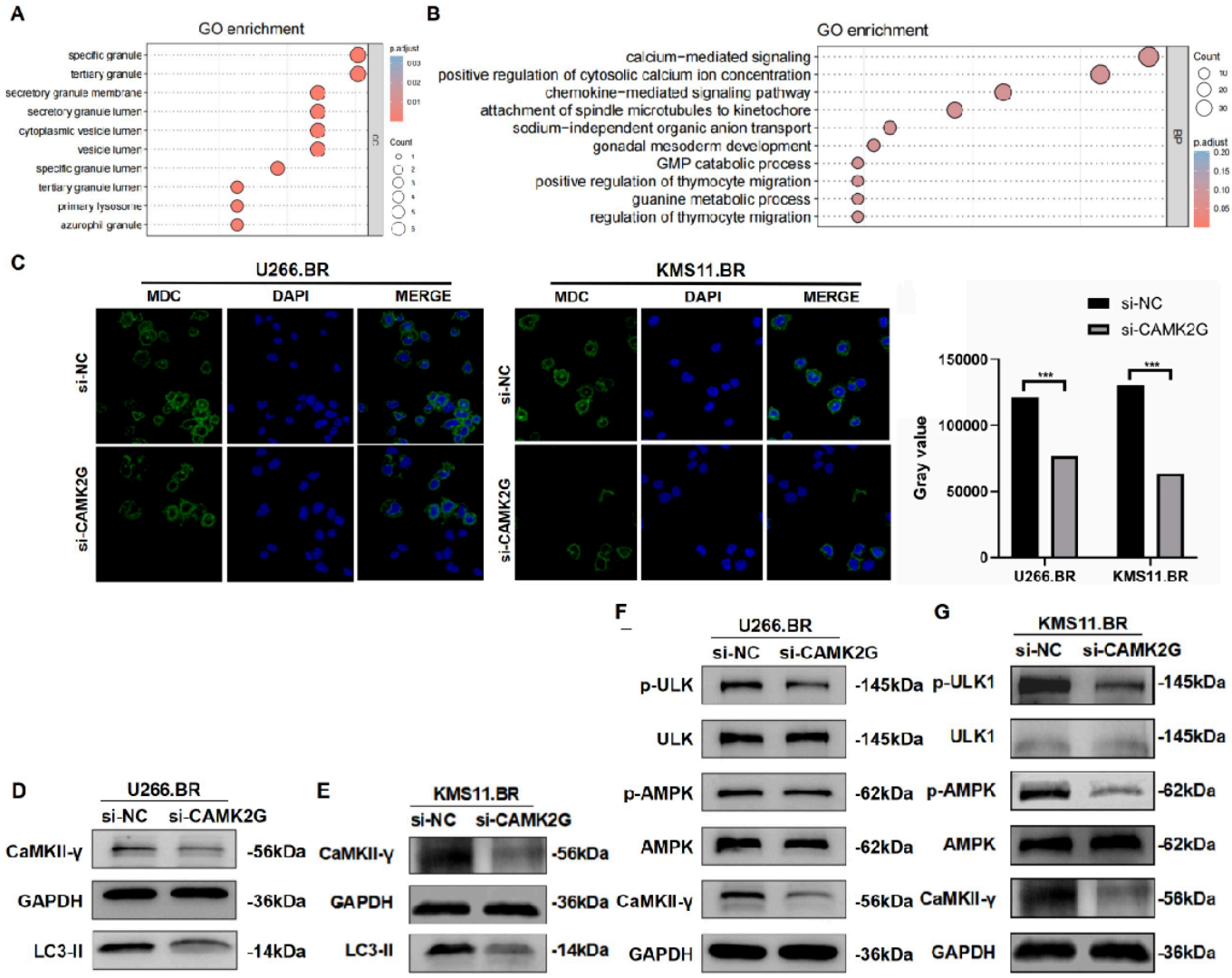
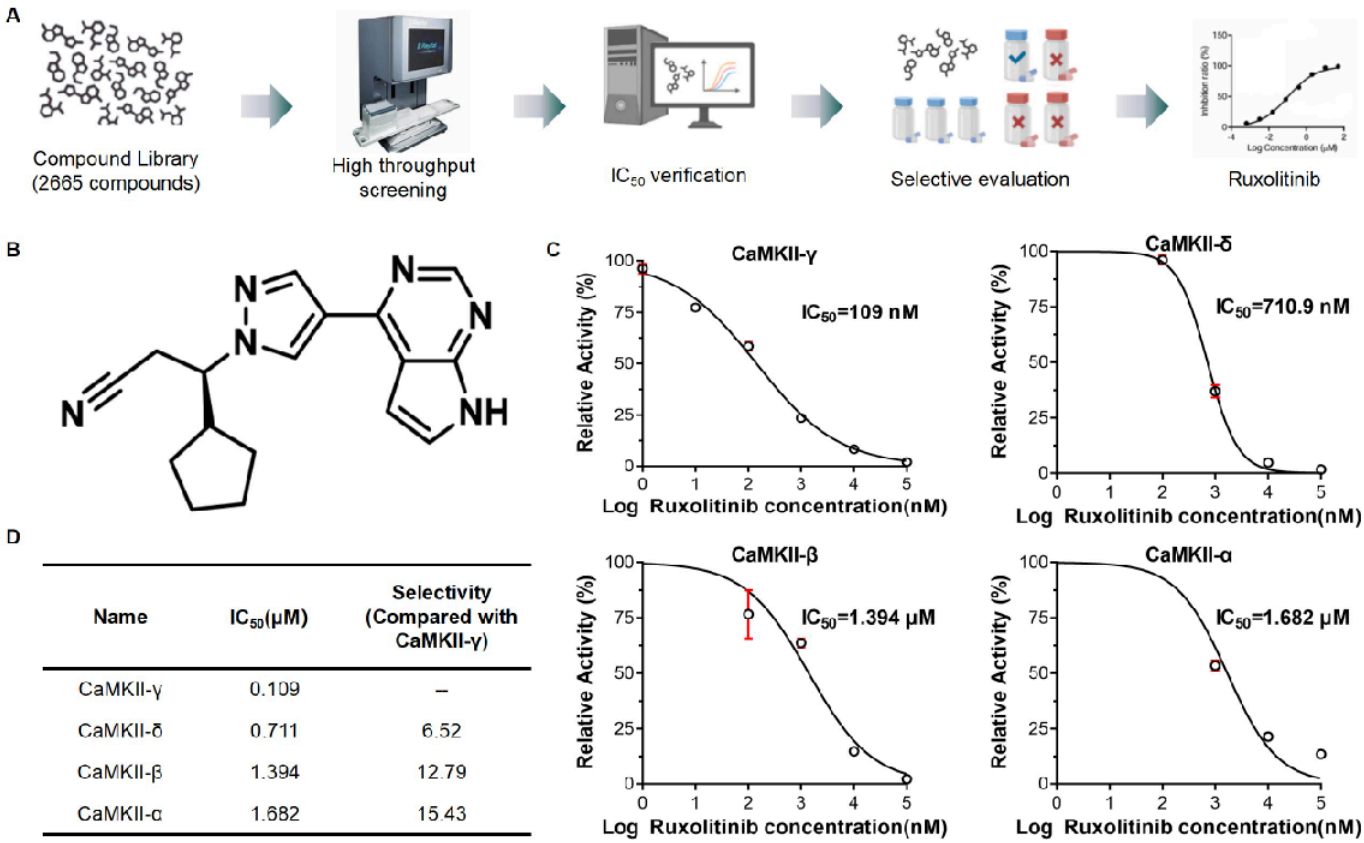


Figure 3

CaMKII-γ regulates autophagy pathway via AMPK-ULK1 axis in BRMM cells. (A) GO enrichment analysis on primary and recurrent MM patients using the MMRFCoMMpass database. **(B)** GO enrichment analysis between high and low expression of CaMKII-γ in recurrent MM patients using the MMRFCoMMpass database. **(C)** Representative images of MDC staining showing autophagic vesicles (green puncta) in U266.BR and KMS11.BR cells with or without CaMKII-γknockdown. **(D-E)** Knocking down of CaMKII-γ by si-CAMK2G in BRMM cell lines (U266.BR and KMS11.BR) resulted in the decrease of autophagic flux. **(F-G)** Knocking down of CaMKII-γ by si-CAMK2G in BRMM cell lines (U266.BR and KMS11.BR) resulted in the down-regulation of autophagy pathway via AMPK-ULK1 axis.



D

Name	IC_{50}(μM)	Selectivity (Compared with CaMKII-γ)
CaMKII-γ	0.109	–
CaMKII-δ	0.711	6.52
CaMKII-β	1.394	12.79
CaMKII-α	1.682	15.43

Figure 4

Discovery of the highly selective CaMKII-γ inhibitor Ruxolitinib. (A) Flowchart of HTS to discover the hit CaMKII-γ inhibitor Ruxolitinib. **(B)** The chemical structure of Ruxolitinib. **(C)** IC_{50} values of Ruxolitinib against CaMKII-α, CaMKII-β, CaMKII-γ and CaMKII-δ determined by kinase activity assay. **(D)** The list of IC_{50} values and selectivity of Ruxolitinib against CaMKII family based on the data in **(C)**.

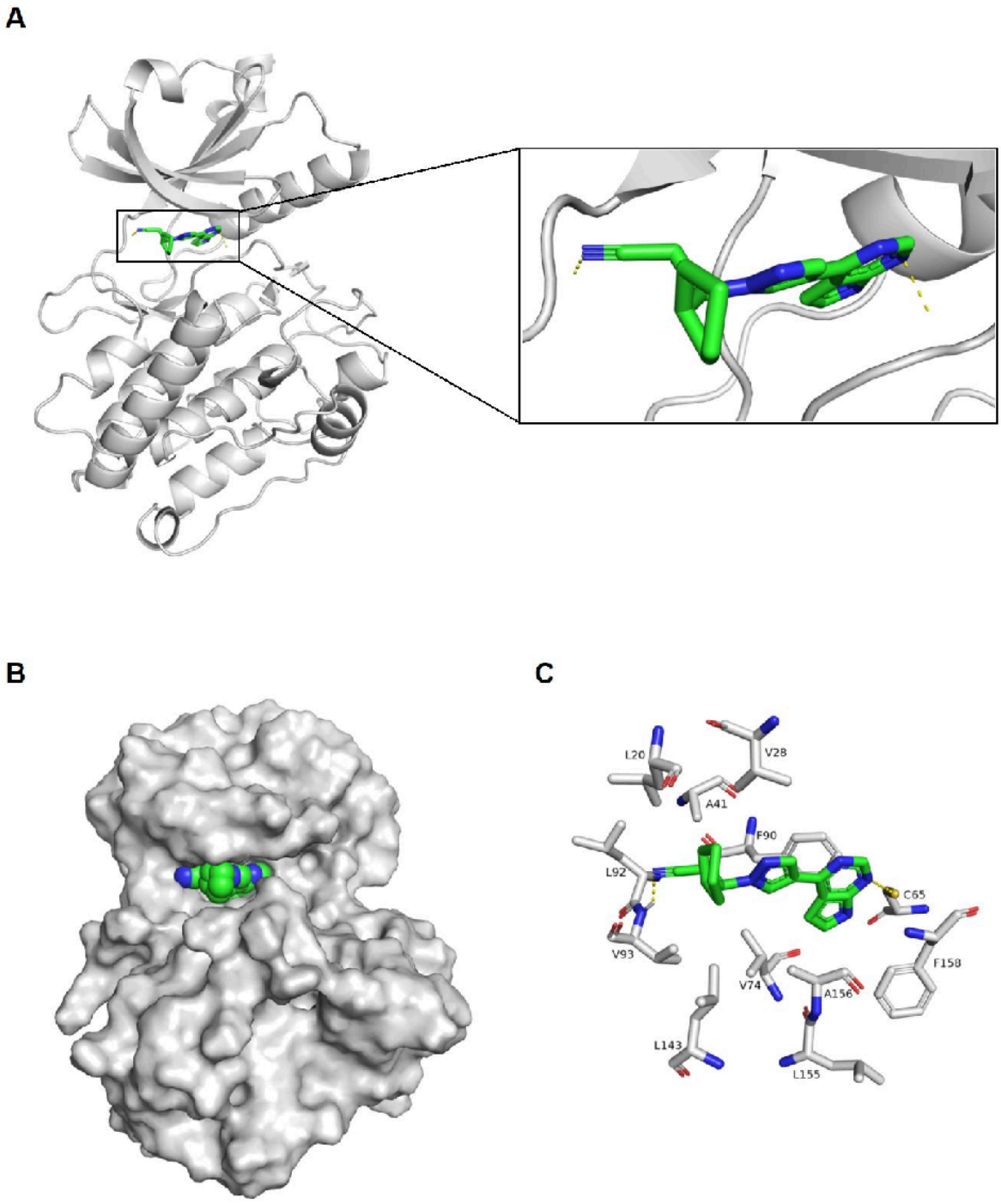


Figure 5

Ruxolitinib binds to the ATP-binding pocket of CaMKII-γ. (A) Molecular docking simulation of CaMKII-γ and Ruxolitinib. CaMKII-γ was shown as ribbons. PDB ID: 2V7O. **(B)**Ruxolitinib occupied the ATP-binding pocket of CaMKII-γ. CaMKII-γ was shown as surface, and Ruxolitinib was shown as sphere. **(C)** Detailed interactions between Ruxolitinib and CaMKII-γ in the docking structure.

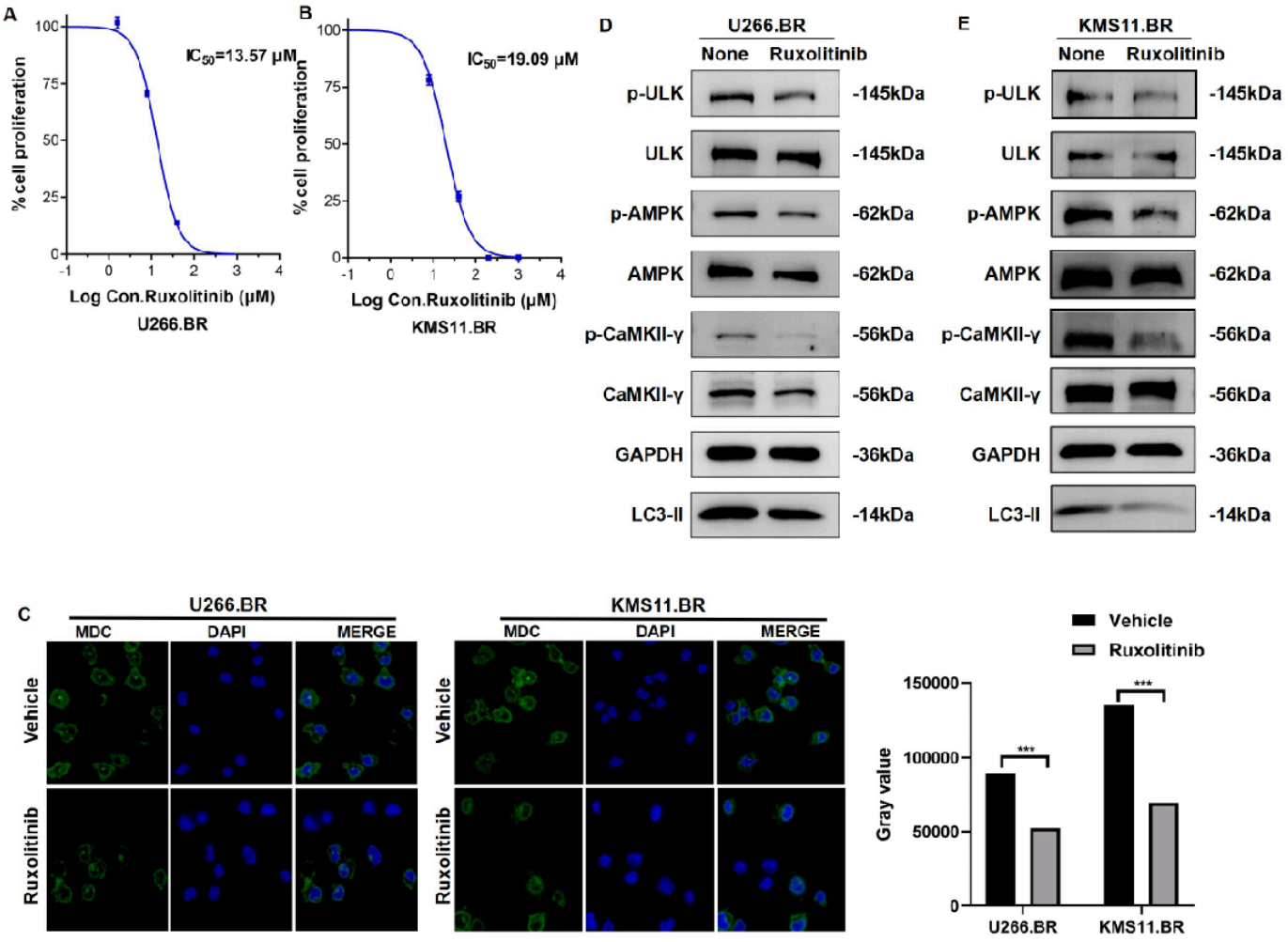


Figure 6

Ruxolitinib inhibits the proliferation of BRMM cells by down-regulating autophagy pathway. (A-B) IC_{50} values of Ruxolitinib against BRMM cell lines (U266.BR and KMS11.BR). **(C)** MDC staining of autophagic vesicles in U266.BR and KMS11.BR cells treated with Ruxolitinib (10 μM) or DMSO for 24 h. Green fluorescent puncta indicate autophagic vacuoles. **(D-E)** BRMM cell lines (U266.BR and KMS11.BR) treated with Ruxolitinib resulted in the down-regulation of autophagy pathway via AMPK-ULK1 axis.

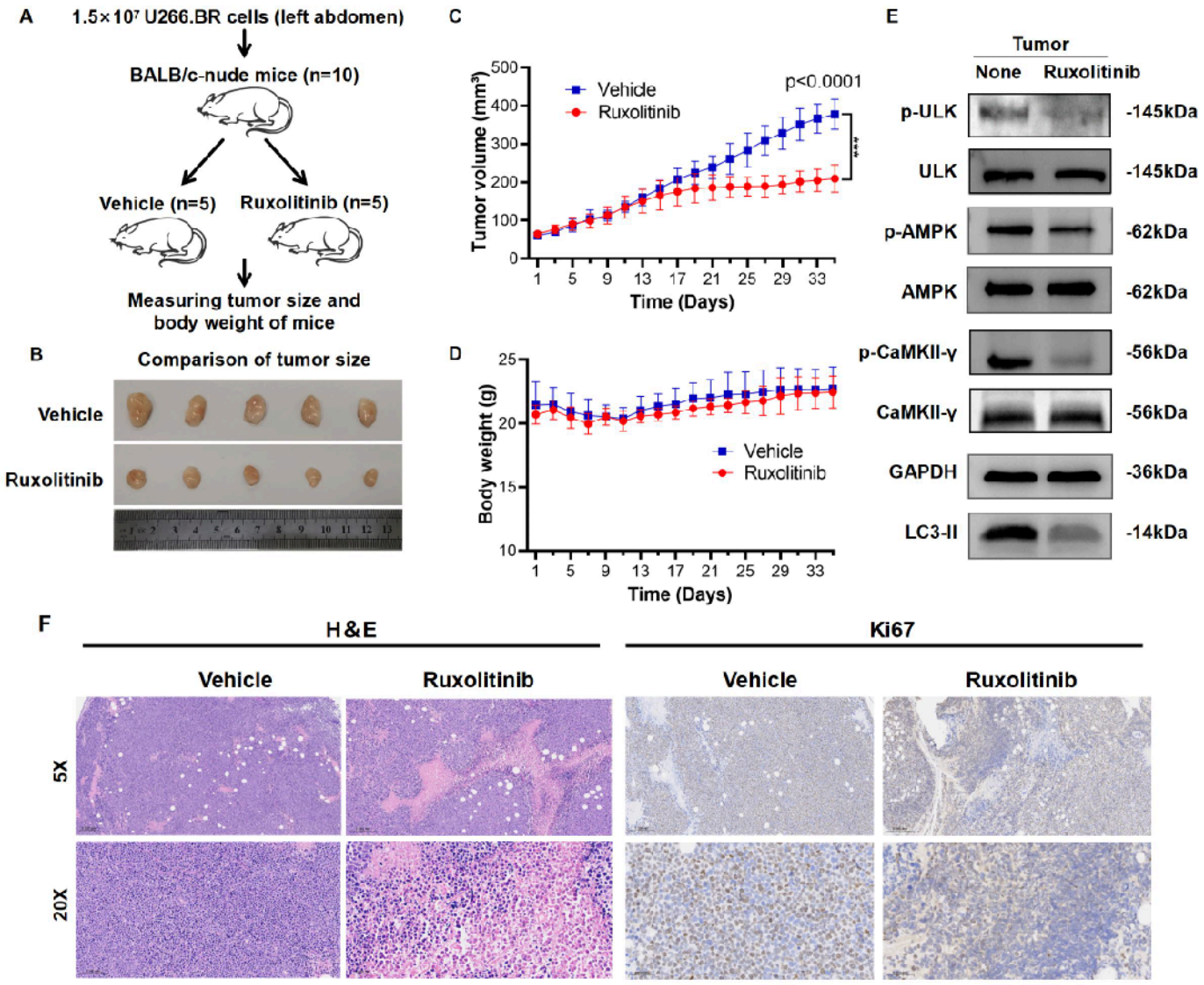


Figure 7

Ruxolitinib demonstrates remarkable anti-tumor activity *in vivo*. (A) BALB/c nude mice received subcutaneous injection of 1.5×10^7 U266.BR cells in the right groin. When tumors grew ~100 mm^3, mice (n = 5/group) were orally administrated vehicle and Ruxolitinib (60 mg/kg) three times a week. **(B)** Tumor tissues of each group were photographed. **(C-D)** Tumor volume and body weight of mice were measured every 2 days. After 35 days, mice were killed. Unpaired two-tailed Student's t test. Error bar, mean ± SD, n = 5. **(E)** The total proteins in the tumor tissues were extracted and used in the western blotting analysis of autophagy pathway via AMPK-ULK1 axis. **(F)** Representative H&E and Ki-67 immunohistochemical staining of tumor sections, showing decreased tumor cell proliferation in the Ruxolitinib group.

Supplementary Files

This is a list of supplementary files associated with this preprint. Click to download.

- TableS1.pdf